Bacillus subtilis as a Novel Biological Repair Technique for Alkali-Activated Slag Towards Sustainable Buildings.

sustainability

MDPI

Article

Bacillus subtilis as a Novel Biological Repair Technique for Alkali-Activated Slag Towards Sustainable Buildings

Nancy Hammad [1], Amr El-Nemr [1] and Ibrahim G. Shaaban [2,*]

[1] Civil Engineering Department, German University in Cairo (GUC), New Cairo 11835, Egypt; amr.elnemr@guc.edu.eg (A.E.-N.)
[2] School of Computing and Engineering, University of West London, London W5 5RF, UK
* Correspondence: ibrahim.shaaban@uwl.ac.uk

Abstract: Rebuilding using outdated methods and tearing down the buildings would have a negative impact on the environment without lowering carbon dioxide emissions or increasing sustainability. This study presents a novel approach to repair that considers environmental and sustainable factors. In contrast to conventional repair methods, the use of *Bacillus subtilis* as an external biological repair technique could offer a novel and sustainable solution, especially when used on alkali-activated slag (AAS) concrete. By breaking down urea into carbonate and ammonium, alkaliphile bacteria can precipitate calcium carbonate. In an environment rich in calcium, the bacteria's opposing cell wall (CO_3^{2-}) draws in positive calcium anions, which result in the formation of calcite crystals. The pores and crevices in the concrete are filled with these crystals. Incorporating bacteria into the fresh mixing of AAS ingredients is contrasted with using *Bacillus subtilis* culture in the water curing medium for pure AAS specimens. The effectiveness of both approaches was evaluated. Direct administration of *Bacillus subtilis* during mixing has a superior outcome regarding mechanical qualities rather than biological therapy, although their effective healing capability in closure of the crack width is similar. The enhancement in compressive and flexural strengths reached 51% and 128% over the control specimens. On the other hand, the healing rate reached nearly 100% for crack widths ranging from 400 to 950 µm. Furthermore, additional studies in this field led to some inferred correlations between the mechanical and durability aspects following healing.

Keywords: alkali-activated slag; self-healing; green construction materials; microbial-induced calcium carbonate precipitation (MICP); bioremediation in concrete; microbial concrete repair; durability enhancement

Academic Editor: Antonio Caggiano

Received: 2 December 2024
Revised: 20 December 2024
Accepted: 22 December 2024
Published: 25 December 2024

Citation: Hammad, N.; El-Nemr, A.; Shaaban, I.G. *Bacillus subtilis* as a Novel Biological Repair Technique for Alkali-Activated Slag Towards Sustainable Buildings. *Sustainability* **2025**, *17*, 48. https://doi.org/10.3390/su17010048

1. Introduction

Sustainability is an important aspect, especially with the new set of visions for 2030 and 2050. The repair with the old technique possesses waste even with these innovative materials, such as FRP sheets, where the FRP sheets and steel pieces would be unused [1,2]. Another aspect that would be more appropriate is the demolishing of the structures that do not maintain any safety and highly degraded concrete where the demolished wastes would be hauled for disposal [1,2]. This action would be influential to the environment by increasing the CO_2 emissions and could not achieve sustainability. Kayan et al. [1] explored low carbon repair techniques for maintaining the heritage structure St Paul's Church within the City of Melaka, Malaysia, based on the materials embodied carbon expenditures. The results reveal that the most sustainable repair techniques are influenced by the lifecycle span of the repair [1]. On the other hand, demolition is another complex

process that has significant environmental implications through systematic tearing down, which can possess waste that can pose serious environmental risks, contaminating soil and groundwater and contributing to landfill use [2]. Besides its footprint, the dust formation contaminates natural spaces and communities, causing health issues and ecological damage due to the vast material volume, which accounts for an energy-intensive 40% of global energy consumption and resource use. Materials reuse and recycling or finding new repair techniques preserve strategic materials that would otherwise be negligible. The environmental and economic benefits of maintaining sustainability are reducing the demand for new materials, conserving natural resources, and lowering the energy consumption associated with manufacturing new products [2,3].

Unfortunately, the concrete's low tensile strength is the first cause of concrete cracking. Tensile stress could be induced through several means, such as excessive external loads, temperature gradient, differential settlement, autogenous shrinkage, drying shrinkage, plastic shrinkage, corrosion, and chemical attacks. Immediate response for crack treatment is pivotal to avoid further crack propagation. Progressive cracking seriously impacts long-term strength and durability [3–7]. Traditional repair is a complicated and resource-consuming process requiring a periodic inspection test, special equipment, and skilled labor. For instance, concrete bridge maintenance and rehabilitation costs reached 4 billion dollars annually in 2014 [8], while 50% of the European annual construction cost is specified for the repair and maintenance of the existing structures [5,6,9]. Another critical issue regarding using traditional repair methods is cement usage [10]. Cement production has prevalent environmental issues associated with subtial carbon dioxide gas (CO_2) emissions. This industry's emission of CO_2 represents around 12% of the global CO_2 emission [11]. In addition to the high consumption rate of natural resources, producing only one ton of OPC consumes one ton of natural resources (lime) [8]. However, epoxy-based repair technology has been widely adopted. Hazardous health problems associated with the produced fume from the epoxy curing process have been reported [8].

On the other hand, the induction of tensile cracks has been indicated in the concrete substrate area because of the different material characteristics [8]. Another challenge is the crack inspection process, particularly for marine structures and tunnels where sophisticated equipment is the only solution. This step may be followed by complicated procedures to reach the inaccessible cracking areas [12]. Thus, it is necessary to introduce an innovative and natural healing technique that can be activated with limited human intervention or even without it [13].

Autogenous and autonomous self-healing technologies have been widely explored within OPC-based concrete with promising results [5,6,14–17]. The microbial-induced calcium carbonate precipitation (MICP) was proposed as a repair approach for healing OPC cracks with reasonable widths up to 970 μm [18,19]. MICP is produced through a subsequential biochemical reaction where urea is decomposed into carbonate (CO_3^{2-}) and ammonium (NH_4^+). The negative charge of the produced carbonate ions attracts the positively charged calcium ions (Ca^{2+}), forming the precipitation of calcite ($CaCO_3$) at the cell surface [14,20,21]. Recent advancements in biological repair techniques for concrete have highlighted the potential of MICP as a sustainable solution for crack remediation. Studies have demonstrated its efficiency in enhancing concrete durability and reducing permeability through self-healing mechanisms [14,17,20,21]. Direct incorporation of bacteria into concrete during mixing has been a focus of research. It has presented several challenges that limit its effectiveness and scalability. The lack of moisture and nutrients in hardened concrete can cause bacterial spores to remain dormant. The second concern is that incorporating bacteria directly during mixing can result in uneven distribution throughout the concrete [14,20]. To overcome these challenges, limited research has investigated the

external application of bacteria as an alternative repair approach. Van Tittelboom et al. [22] compared repair techniques, such as epoxy, grout injection, and bacteria technology in OPC concrete. The results proved that cement grouting only covered the surface without filling the crack due to the large grain size of the grout. By contrast, epoxy and bacteria treatments led to a complete filling. Bacterial treatment was almost as good as epoxy treatment for cracks with a depth of less than 10 mm [22].

A further study performed by Prayuda et al. [23] showed that incorporating *Bacillus subtilis* in the curing water for 28 days healed microcracks of OPC beams and restored the flexural strength by about 93.63%. It is worth mentioning that aside from the crack healing, the addition of bacteria improved the strength and durability of the whole composite. For instance, Ramakrishnan et al. [24] reported an increase of 18% in the 28-day compressive strength by adding *Bacillus pasteurii* to OPC concrete. Nosouhian et al. [25] stated a 20% improvement in compressive strength with the addition of *Bacillus subtilis* when compared with the control OPC concrete. The improvement in the compressive strength was accompanied by a 30% increase in the chloride resistance. Another type of *Bacillus subtilis*, known as *Bacillus sphaericus*, was confirmed to positively influence compressive strength by 36%, along with an improvement in the water absorption of the OPC mortar [18]. Balam et al. [26] indicated that incorporating *Sporosarcina pasteurii* enhanced chloride resistance by 34%. Despite the successful method followed by Prayuda et al. [23] for incorporating bacteria in the curing medium for OPC concrete repair, most researchers focused on incorporating bacteria during the fresh concrete mixing. Additionally, using microbial solutions as a crack repair technique was not previously addressed with alkali-activated slag (AAS) systems. In this study, the slag has been selected as it does not require any other treatment such as heat curing to elevate its activation like the one presented by the fly ash. In addition, heat curing might not be the appropriate combination for the bacteria to survive within media for further activation. Incorporating *Bacillus subtilis* in the curing medium for external crack healing of AAS composites was evaluated in this study. The evaluation occurred by examining the mechanical properties, durability, and microstructure analysis. The assessment process involved comparing the influence of applying *Bacillus subtilis* in the curing water and the influence of immobilizing bacteria during the fresh mixing of the AAS mixture materials. This investigation is maintaining sustainability by utilizing materials eco-friendly to the environment while searching for suitable techniques of repair in the case of utilizing concrete-based AAS. This research effectively tackles key challenges in AAS production and performance as well, and it represents a groundbreaking contribution to the development of practical and sustainable solutions.

2. Experimental Program

2.1. Materials

Ground granulated slag with the chemical composition of SiO_2 of 35.40%, CaO of 36.87%, and Al_2O_3 of 17.40% (see Table 1) was adopted in this study. The slag fineness was 4088 cm^2/g, with a specific gravity of 2.80. The chemical modulus of this type of slag that is represented in the summation of silicon oxides and calcium oxides is 72.27%, which is greater than 70% alongside aluminum oxides less than 20%. Thus, this binder is considered as moderately calcium oxide, as reported by Palomo et al. [3]. Upon activation, it could produce a binding gel with appropriate strength and durability [3,4]. Consequently, slag has emerged as a cement replacement in alkali-activated slag concretes, road bases, soil stabilization, and precast products [3,4]. The activated alkaline activator was a blended solution of sodium meta-silicate (Na_2SiO_3) and sodium hydroxide (NaOH). The percentages of sodium oxide, silicon oxide, and water within the sodium silicate solution were 27%, 30.01%, and 59.72%. Sodium hydroxide solids (flakes) weights in the solution represented

37.2%. The NaOH flakes were dissolved in water for 24 h before mixing for exothermic heat release.

Table 1. Chemical composition of slag.

Oxides	%
SiO_2	35.40
CaO	36.87
Al_2O_3	17.40
MgO	6.83
MnO	0.26
Fe_2O_3	1.4
MnO	0.35
TiO_2	0.11
S	0.24
L.O.I	0.50

Figure 1 represents the *Bacillus subtilis* culture prepared with the target cell concentration of 10^5 cells/mL. The alkaliphile *Bacillus subtilis* is a resilient spore-forming bacterium with the ability to survive as spores. These spores remain dormant until cracks form and moisture activates them, triggering calcite precipitation to heal cracks [27]. This type of bacteria could survive within alkaline environments such as concrete, which has a high pH (ranging from 12 to 13). The selection of *Bacillus subtilis* was attributed to their greater resilience to alkaline conditions than other bacteria [27]. The microbial sample of *Bacillus subtilis* was performed at the Faculty of Science of Al-Azhar University, Cairo, Egypt, similar to those prepared by Shaaban et al. [17]. The *Bacillus subtilis* sample preparation is summarized as follows: the bacteria were cultured in a formulation composed of 1% tryptone, 0.5% yeast extract, 1% NaCl, and 1.5% agar. The second step was sterilizing all glassware and instruments for 20 min, which was an important step to avoid contamination by other species. The inoculation process included preserving bacteria for 24 h at 37 °C.

Figure 1. *Bacillus subtilis* culture.

A spectrophotometer was used to determine the optical bacteria density required to prepare a microbial culture of a cell concentration of 10^5 cells/mL. Subtilis absorbance was determined through a qualitative procedure depending on measuring the optical density of spore suspension at 600 nm (OD600). The germination process was checked every 24 h to spot the OD600. A colony-forming unit per milliliter (CFU/mL) was used to determine the

microbes' growth rate. The OD and CFU/mL measurements were repeatedly recorded up to 0.1 OD to spot the required concentration level. Table 2 indicates the main characteristics of the microbial culture. It should be mentioned that the supernatant was then centrifuged at 10,000 rpm at a pH of around 10.5 and the bacteria produced complied nearly with those provided by *B. subtilis* strain 168 (ATCC, Manassas, VA, USA). The bacteria and culture medium were prepared and tested for pH, etc., as mentioned earlier outside the civil laboratory of the German University in Cairo, as shown in Figure 1.

Table 2. *Bacillus subtilis* culture characterization.

Characteristics of *Bacillus subtilis*	Value
Growth medium	3
Incubation time	24 h
Subculture	30 days
Gram stain	Positive
Shape	Rod
Oxygen demand	Facultative

2.2. AAS Mortar Manufacture

The manufacturing process started by blending the alkaline solutions. Sodium metasilicate solution was mixed with sodium hydroxide solution after 24 h of sodium hydroxide solution preparation. The alkaline activators were added to specific water content based on the liquid-to-solid ratio (L/S) involved in the mix design. The slag and the solution weights were determined per the absolute volume method alongside the equations of modulus silicates (Ms), alkali dosage (Na_2O%), and L/S, as illustrated in Equations 1–4. According to the Egyptian Code of Practice (ECP) [28], the ratio between slag and sand was kept to 1:3. The solid ingredients were adequately mixed for 3 min in a 5-L Hobart mixer. The blended solutions were added gradually and mixed with the solid constituents for 2 min. For the AAS mix with direct bacteria application during mixing (mix C-5), another 2 min were considered upon adding the microbial culture.

Then, the prepared AAS mortar was poured into the metallic molds and de-molded after 24 h. AAS specimens were subjected to air curing for 7 and 28 days, except the specimens of mix C-5. These specimens were subjected to water curing to maintain microbial survival [29]. Specimens were subjected to pre-cracking, evaluating the influence of bacteria on the crack healing. Pre-cracking took place by applying a compression load of up to 85% of the ultimate load [6,17]. Photo documentation was obtained to assess the damage and healing amount. The cracked pure AAS specimens were subjected to water curing incorporating *Bacillus subtilis* culture with a cell concentration of 10^5 cells/mL. The AAS specimens with the direct bacteria addition were immersed in pure water for 7 and 28 days during mixing. Based on the literature [30–33], the bacteria cell concentration of 10^5 cells/mL had the optimum influence on the mechanical and durability properties. For that, the concentration of the adopted microbial culture was kept at 10^5 cells/mL. Figure 2 illustrates the different techniques for the bacteria applications and curing conditions handled through the flow chart, explaining the whole process adopted in the experimental program.

$$\frac{\text{Slag}}{SG_{slag}} + \frac{Na_2SiO_3}{SG_{Na_2SiO_3}} + \frac{NaOH}{SG_{NaOH}} + \frac{H_2O}{SG_{H_2O}} = 1000\ \text{L} - \frac{CA}{SG_{CA}} - \frac{FA}{SG_{FA}} \quad (1)$$

where slag is the slag weight in kg; Na_2SiO_3 represents the sodium silicate content in kg; the weight of sodium hydroxide in kg is indicated in NaOH; H_2O shows the weight of the water content in kg; CA and FA are the weights of coarse and fine aggregates in kg, respectively; and SGx is the specific gravity of the corresponding material x.

$$Na_2O\% = \frac{Na_2O\% \text{ in NaOH} + Na_2O\% \text{ in } Na_2SiO_3}{\text{Mass of slag}} \quad (2)$$

$$Ms = \frac{SiO_2\% \text{ in } Na_2SiO_3}{Na_2O\% \text{ in } Na_2SiO_3 + Na_2O \text{ in NaOH}} \quad (3)$$

$$L/S = \frac{\text{Water in all solutions}}{\text{Slag} + Na_2O\% \text{ solids} + SiO_2 \text{ solids}} \quad (4)$$

where $Na_2O\%$ in NaOH and $Na_2O\%$ in Na_2SiO_3 represent the percentages of sodium oxide solids in the NaOH and Na_2SiO_3 solutions, respectively; $SiO_2\%$ in Na_2SiO_3 is the percentage of silicon oxide solids in the Na_2SiO_3 solution; water in all solutions is the water percentage in the AAS mixture.

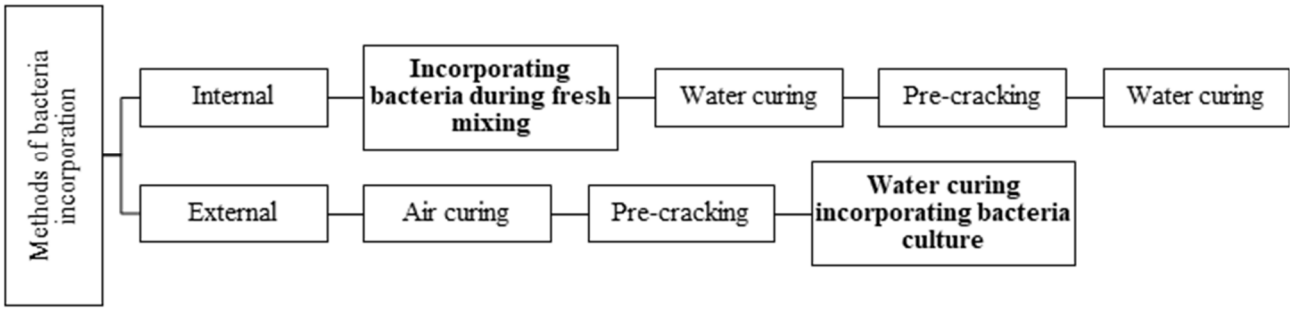

Figure 2. Flow chart illustrating different microbial techniques adopted in the experimental program.

Table 3 highlights the mix proportions adopted in the experimental program of this investigation. Mix "C-A" refers to the pure AAS control mix with normal air curing conditions; "C-5" indicates immobilizing bacteria directly during the fresh mixing and using water curing conditions for bacteria activation. Incorporating *Bacillus subtilis* in curing media for crack repair is presented in the mix "C-B." After several laboratory trials, the AAS mix was selected to reach an appropriate mix with proper compressive strength, flowability, and setting time. The flow diameter and initial and final setting times of the AAS mix were 100 mm and 82 and 180 min, respectively.

Table 3. Designated AAS mixes proportions.

Mix ID	Slag kg/m^3	NaOH kg/m^3	Na_2SiO_3 kg/m^3	H_2O kg/m^3	$Na_2O\%$	Ms	L/B	Bacteria Concentration Cells/mL	Curing Medium
C-A	387.40	60.45	82.81	81.61	8%	0.8	0.38	-	Air
C-5	387.40	60.45	82.81	81.61	8%	0.8	0.38	10^5	Water
C-B	387.40	60.45	82.81	81.61	8%	0.8	0.38	-	Bacteria

2.3. The Assessment Technique

Mechanical tests, mainly compressive and flexural strength tests, were conducted on AAS specimens after 7 and 28 days. The compression and flexural tests were performed using a Universal testing machine of capacity 2000 kN as per the specifications of ASTM C109 [34] and ASTM C348 [35], respectively. Then, 40 mm-mortar cubes were compressed at 240 kg/m^3 per minute pacing rate. A three-point loading flexural test was applied on mortar prisms of 40 × 40 × 160 mm with a loading rate of 50 N/s. The final recorded strength was the average of three specimens from each mixture at the requested testing age. The enhancement in compressive and flexural strengths was captured by the following Equation (5) [36].

$$\text{Enhancement in compressive/flexural strength } (\%) = \frac{\sigma_b - \sigma_c}{\sigma_c} \quad (5)$$

where σ_b is the compressive/flexural strength of microbial mortar samples and σ_c is the compressive/flexural strength of control samples.

The durability properties, including water absorption, porosity, and chloride attack resistance, were evaluated to check the bacteria's effectiveness in precipitating calcite crystals in the AAS specimens' pores. Water absorption and porosity tests were carried out at 28 days of age on cylindrical discs of 100 mm diameter and 50 mm thickness according to ASTM C642-21 recommendations [37]. The Rapid Chloride Permeability Test (RCPT) was performed based on the specifications of ASTM C1202 [38] and AASHTO–T277 [39] to evaluate the chloride attack resistance. The test was initiated by inserting the cylindrical specimen in a vacuum desiccator. A pressure of less than 6.65 kPa was maintained in this phase for 3 h. Then, specimens were kept under de-aerated water in the RCPT cell for 182 h without allowing air access. After that, one end of the circular disc was immersed in a 3% sodium chloride solution, while the other side was subjected to a 0.3 M sodium hydroxide solution. Passing charges with 60 V were applied across the two ends. The current passing through the specimens was determined at specific time intervals for 6 h. The chloride resistance was evaluated based on the total charges computed in Coulombs.

For capturing the healing progress of the AAS specimens, whether they were directly incorporating bacteria during mixing or being subjected to bacteria culture as a repair technique, scanning electron microscopy (SEM) equipped with Energy Dispersive X-ray analysis (EDX) was applied. Further, an X-ray diffraction test was performed to detect the formation of the produced chemical compounds, specifically the calcium carbonate crystals, as shown in Figure 3.

(**a**) (**b**) (**c**)

Figure 3. AAS manufacturing process in its (**a**) fresh state, (**b**) hardened state in terms of AAS specimens, and (**c**) pre-cracking cube specimen.

3. Results and Analysis

3.1. Compressive Strength

The results of the direct bacteria incorporation during fresh mixing (as in mix C-5) showed a remarkable enhancement in the 28-day compressive strength that reached 51.28% compared to the control mixture (C-A), as shown in Figure 4. This significant improvement was attributed to the precipitation of calcite crystal within the internal pores and fissures of the AAS composite [40] in mix C-5. The positive influence of incorporating bacteria on the compressive strength of OPC was previously pointed out in several studies [17,25,27,41–46]. Some scholars tested the incorporation mechanism on the efficiency of the induced microbes such as *Sporosarcina pasteurii* [47,48], *Bacillus subtilis* [24,27], *Bacillus cohni* [41], *Bacillus megaterium* [42], and *Shewanella* [43]. The mentioned incorporation methods were direct and indirect mechanisms. The direct mechanism means that the microbes are directly added during mixing [17,25,47]. Upon direct addition, the reaction process tends to decrease the viability of the bacteria cells. However, the spores-bacterial type could be provided as

an efficient solution. Spore-bacterial type is a positive-gram alkali-resisting bacteria with the ability to spore-form in an inactive form, which can be activated upon exposure to water. The *Bacillus* family is an example of spore-forming bacteria [14,22]. The second method depends on immobilizing the bacteria in another material called a carrier, such as cement stone [41], zeolite [48], lightweight aggregate [27], and hydrogel [24]. Nevertheless, a leakage of bacteria from the carrier has been reported in such cases. The influence of incorporating different types of bacteria by adopting the direct and indirect mechanisms on the compressive strength is shown in Figure 5. Both methodologies indicated a positive effect on compressive strength, which figured out the intense microbiological activity required to precipitate calcium carbonate within concrete under different conditions.

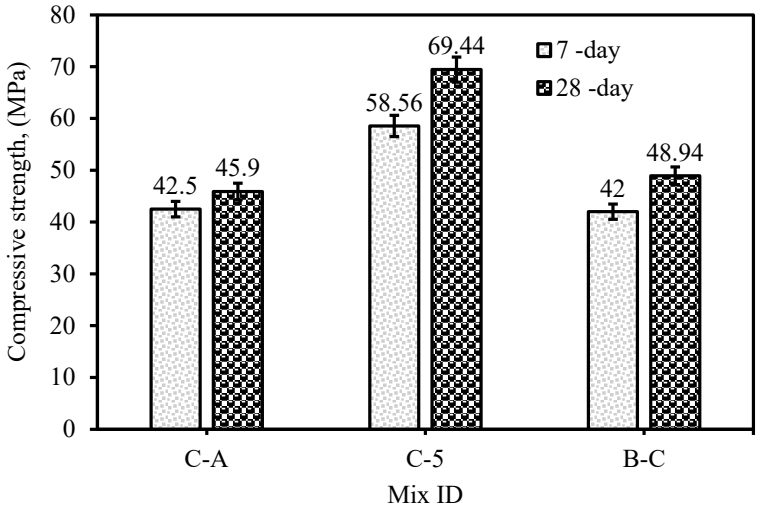

Figure 4. Compressive strength of the AAS specimens at 7 and 28 days for different adopted mechanisms in this investigation.

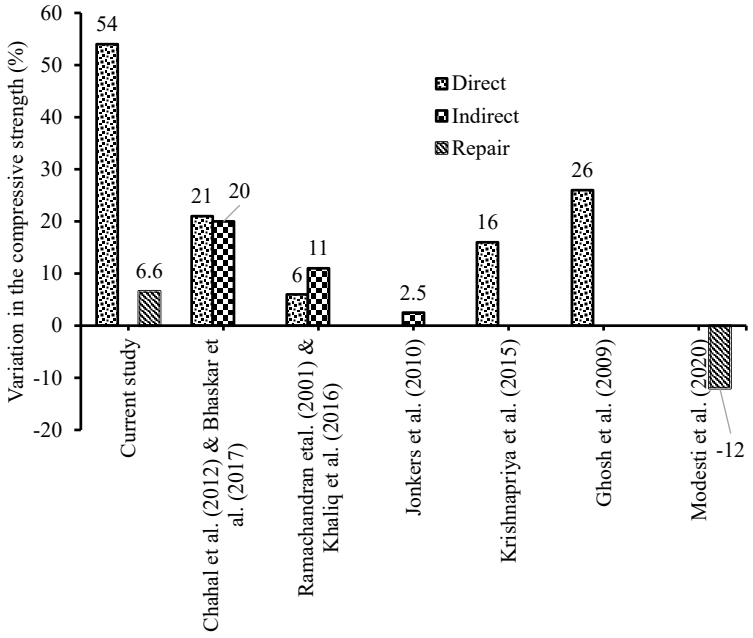

Figure 5. The influence of different healing mechanisms/species as *B. subtilis* (Current study), *S. pasteurii* [47,48], *B. subtilis* [24,27], *B. cohnii* [41], *B. megaterium* [42], *Shewanella* [43], and *Epoxy* [49] on compressive strength. [24,27,41–43,47–49].

The adopted microbial suspension repair technique did not substantially change the developed compressive strength after 7 or 28 days of curing. The compressive strength was almost the same as that of the specimens cured 7 days in the air, which had a value of

42.0 MPa. There was a slight increase in the 28-day compressive strength with an increment of 6.6% for specimens cured in bacteria solution (increased from 45.9 MPa to 48.94 MPa). The same observations were stated by Prayuda et al. [24], where the only increase in compressive strength of OPC specimens cured in *Bacillus subtilis* suspension after 28 days was limited to 2.1%. This behavior is attributed to exposing the external surface only of specimens to the bacteria solution where the outer pores were filled with calcium carbonate precipitation; however, the still internal matrix includes the pores generated through the microcracks that occurred. Despite the slight increase in the compressive strength, this mechanism achieved promising results compared to epoxy adhesives. Epoxy was reported to adversely affect the concrete compressive strength [49,50]. Several parameters could explain this observation; the first crucial point is the bond strength between the old concrete and the adhesive material, where each material has different physical and mechanical properties. The variation in the material's characteristics causes differential shrinkage. The new repair material undergoes early-age shrinkage, while the old composite has already proceeded with this phase. Hence, the interface area has become easily subjected to additional tensile stresses that reduce the resisting capacity [8]. Furthermore, the quick setting time of the epoxy adhesive (15–30 min) and the fast-heating rate could highly affect the resin's viscosity and compressive strength. Consequently, Modesti et al. [49] reported an average reduction in concrete's ultimate compressive strength of 8.87%.

3.2. Flexural Strength

A considerable change in the flexural strength behavior was reported, where the flexural strength improved by 143% and 128% for AAS specimens with direct bacteria incorporation (C-5) after 7 and 28 days, respectively, compared to the air-curing specimens. For the external bacteria curing, the enhancement in the flexural strength was recorded at 87.2% and 67.0% for 7 and 28 days, respectively, as shown in Figure 6. Flexural strength is sensitive to the crack's direction. Shrinkage cracks could propagate perpendicularly to the flexural-induced tensile stress (transverse direction), reducing the localized resisting area at the critical crack tips [44,51]. Unlike compressive strength, the influence of shrinkage cracks is not profound due to the propagation direction in which the compressive cracks are parallel to the shrinkage cracks. By healing these cracks, a significant enhancement was recorded in the flexural strength due to filling the internal and external AAS micro-pores. This phenomenon was realized by Fang et al. [51]. This behavior was found in harmony with the findings reported by Reddy et al. [44], who compared the flexural strength of OPC specimens cured in *Bacillus subtilis* solution with the corresponding specimens cured in water, where the increase in the flexural strength was 67% after 28 days of curing.

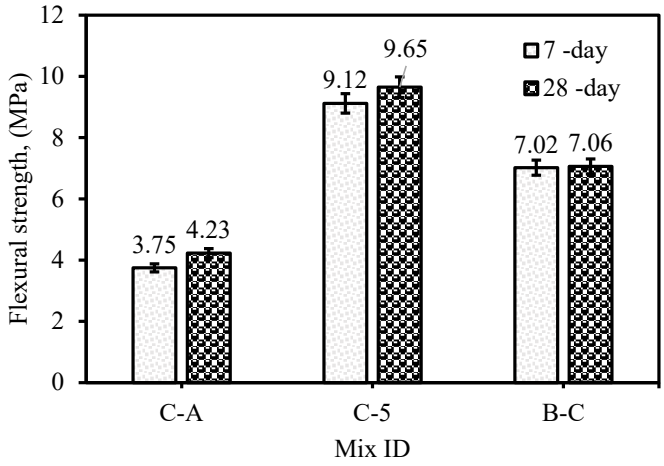

Figure 6. Flexural strength of the AAS specimens at 7 and 28 days.

3.3. Relationship Between the Mechanical Properties

This section discussed a relationship between mechanical properties such as compressive and flexural strengths after healing. Table 4 shows the flexural strength ratio for the specimen after repair utilizing the healing bacteria in both cases relative to the compressive strength. The ratio showed 9, 13.9, and 14.43% for the C-A, C-5, and B-C mixes at 28 days of age. The ratios were also deduced at 7 days relevant to the compressive strength. The values provided higher ratios than those 28 days. The ratios provided 8.82, 15.57, and 16.71%, respectively.

Table 4. Strength ratios of repaired AAS.

Mix ID	f_t/f_c (%)	
	7 Days	**28 Days**
C-A	8.82%	9.22%
C-5	15.57%	13.90%
B-C	16.71%	14.43%

Further investigation is required to predict the flexural strength relevant to compressive strength enhancement. If the existing equations in the code and guidelines (Table 6 in [52]) were utilized, the square root of the compressive strength would be multiplied by 1 or nearly 0.99 factors, which is not the case in Ordinary Portland Concrete. So, it is imperative to maintain a predictive model for further correlating the flexural and compressive strength and the elastic modulus of stiffness of the AAS to maintain the integrity and check the repaired structural element soon. It is worth noting that the low coefficient of determination is attributed to the sample size. The data size is an obstacle, but the idea of visiting this area is very important for future work for investigation.

3.4. Water Absorption and Porosity

Water absorption and porosity evaluation are mainly correlated to pores within the paste, the aggregate, and the interfacial transition zone (ITZ) between the paste and the aggregate. These tests aimed to assess the calcite precipitation formation within the pores or the cracks that appeared in the ITZ and/or the paste itself. The incorporation of direct bacteria spores during mixing achieved better results of 42.0% and 32.1% improvement in water absorption and porosity, respectively, compared to the external curing application. The microbial solution curing technique enhanced the water absorption by 21.5% and the porosity by 28.9%, as illustrated in Figure 7. *Bacillus subtilis* was proved to have the ability to convert urea into ammonium and carbonate and promote the microbial deposition of carbonate into calcium carbonate even when it was applied externally. These findings are compatible with the literature [25,45–47,53]. Multiple studies focused on the influence of incorporating bacteria on water absorption and porosity results [25,45,46,48,53]. The same level of improvement was reported for immobilizing various types of bacteria, such as *Sporosarcina pasteurii* [48] and *Bacillus aerius* [45], in OPC mortar. Figure 8a,b highlights the induced microbes' positive effect on improving OPC's physical properties. The recorded enhancement was between 15–46% and 14–55% for water absorption and porosity, respectively [25,45,46,48,53]. For instance, Siddique et al. [46] reported a decrease in the water absorption and porosity with direct inclusion of the ureolytic bacteria with a concentration of 10^5 cells/mL by 23.1% and 16.9%, respectively. It is essential to mention that these studies considered only the direct microbe inclusion during the OPC mixing [25,45,46,48,53]. This study shed light on the applicability of externally applying bacteria to curing water. Despite the lower effectiveness of this procedure, this could be a pivotal step for adopting a novel biological repair technique. The ureolytic bacterial solution effectively enhanced the

external surface, indicating calcium carbonate crystals forming on the external specimen surface rather than the internal pores when the bacteria solution is in water curing.

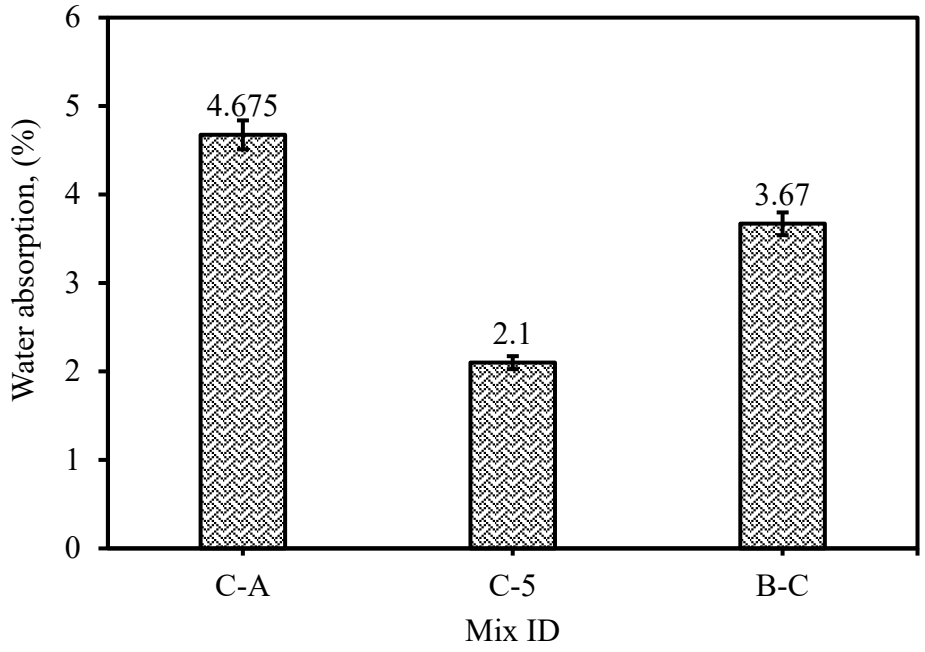

(**a**)

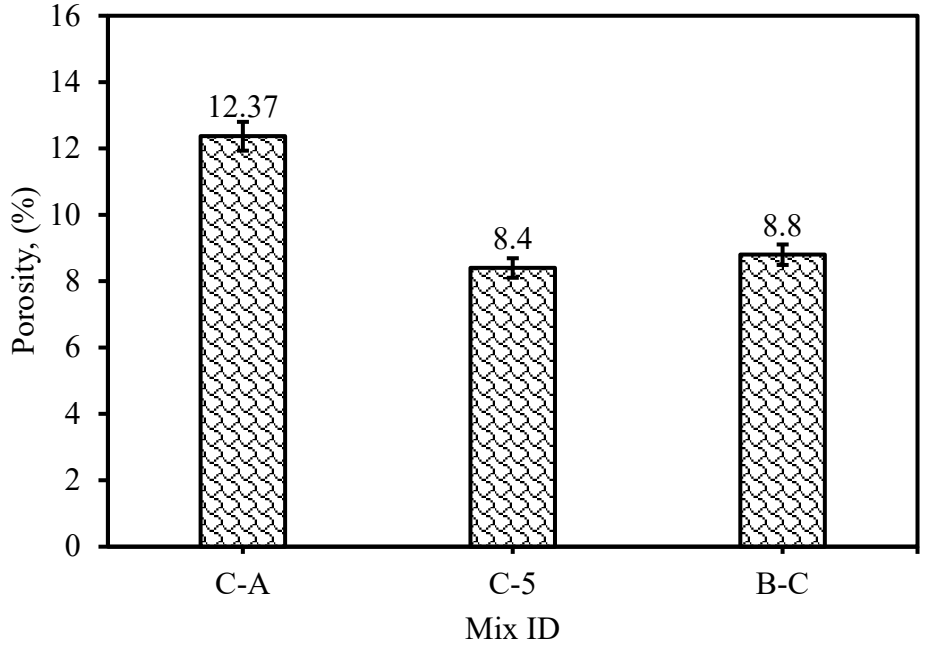

(**b**)

Figure 7. The influence of bacteria on the (**a**) water absorption and (**b**) porosity of the AAS mixes.

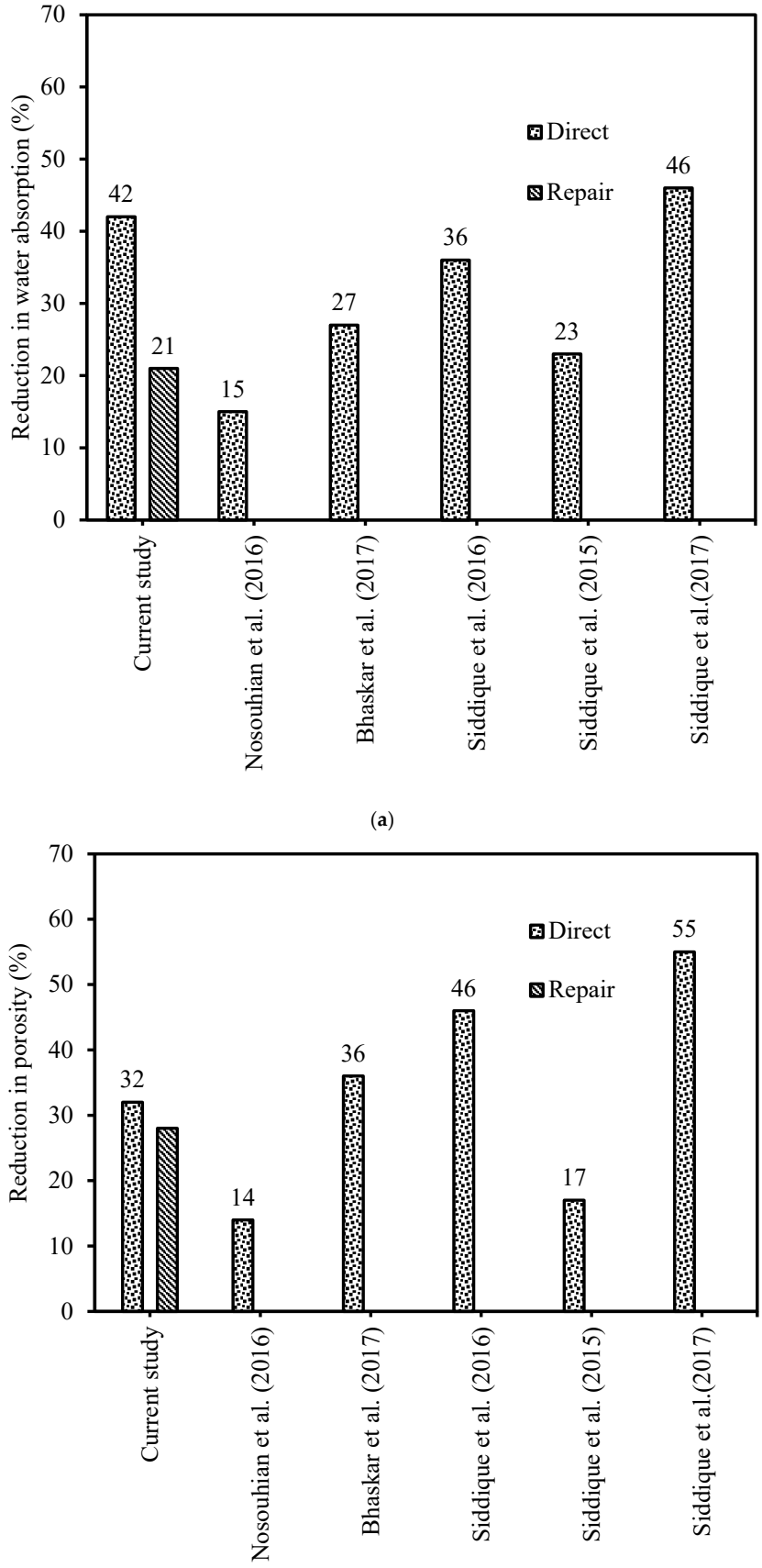

Figure 8. The influence of the healing agent *B. subtilis* (Current study) and other species on (**a**) water absorption and (**b**) porosity [25,45,46,48,53].

3.5. Rapid Chloride Permeability Test (RCPT)

Pore structure and porosity are among the crucial parameters controlling chloride resistance behavior. Chloride ions could be easily transferred through more significant pores. The narrower pore structure hinders the transportation of Cl^- ions, increasing the composite resistance. AAS systems are generally characterized by a high-fineness binder with high calcium content that produces a denser pore structure. However, it is worth pointing out that the pore solution of AAS systems activated by alkaline solutions is more complicated than the OPC matrix due to more mobile ions Na^+, OH^-, and HS^- [54–57]. This behavior is the main reason for the sudden stoppage while applying the RCPT test on the other AAS specimens after 120 min for AAS mixes C-A and C-5. Excessive mobile ions Na^+, OH^-, and HS^- led to higher passages of the electric charges, reflecting false results even in the C-5 specimens. This action was noted by multiple scholars, such as Balcikanli and Ozbay [58] and Hu et al. [59], who confirmed that the accelerated electrical conductivity recorded during the RCPT was due to the high concentration of the alkaline activators. However, the number of passing charges dramatically decreased in the case of C-5 compared to the reference specimens C-A. Some mobile ions were consumed during the microbiological reactions, reducing the available free ions, and the charges passed, reflecting lower penetration.

For the specimens cured in the microbial solution C-B, there was a significant improvement in the specimen's chloride attack resistance. The first achievement was the completion of the RCPT to reach the required 6 h of chloride resistance. The second was that the number of passing electrical charges reduced significantly to 1214.78 Columbus after 360 min with a corresponding current of 17 Amperes, as illustrated in Figure 9. Also, it should be mentioned that Table 5 was added to provide values of Figure 9. Based on these observations, the microbial-cured AAS specimens could be classified as a perfect material resistant to chloride attack, according to ASTM C1202 [38]. The continuous submergence of specimens in the microbial suspension led to better exposure of the outer surfaces to the immobilized bacteria. This condition facilitated the biochemical ureolytic reactions, microbial-induced calcium carbonate precipitations on the external pores, and shrinkage-induced microcracks. By blocking the external pores and microcracks, the transmission of mobile ions was hindered, reflecting lower passing electrical charges and lower chloride conductivity. This behavior agrees with Tittelboom et al. [22] and Prayuda et al. [23], who confirmed the effectiveness of applying microbial suspension as a curing regime for crack repair in OPC concrete specimens. It is essential to mention that AAS is characterized by its high chloride attack resistance, supported by multiple studies [57–59]. At the same time, other types of tests (ponding tests) were performed. The RCPT's misleading results in testing the C-A and C-5 specimens emphasized the need for modifying RCPT to cope with the nature of the AAS chemical composites.

Table 5. The RCPT values for the mixes.

	T (min)	**0**	**30**	**60**	**90**	**120**	**150**	**180**	**210**	**240**	**270**	**300**	**330**	**360**
C-A	Q (c)	260	919	1908	3253									
	I (ma)	260	386	601	621									
C-5	Q (c)	124	443	777	1080									
	I (ma)	138	177	185	168									
C-B	Q (c)	88	291	512	730	862	946	1007	1056	1098	1135	1169	1200	1214
	I (ma)	98	113	122	121	73	46	33	27	23	20	18	17	16

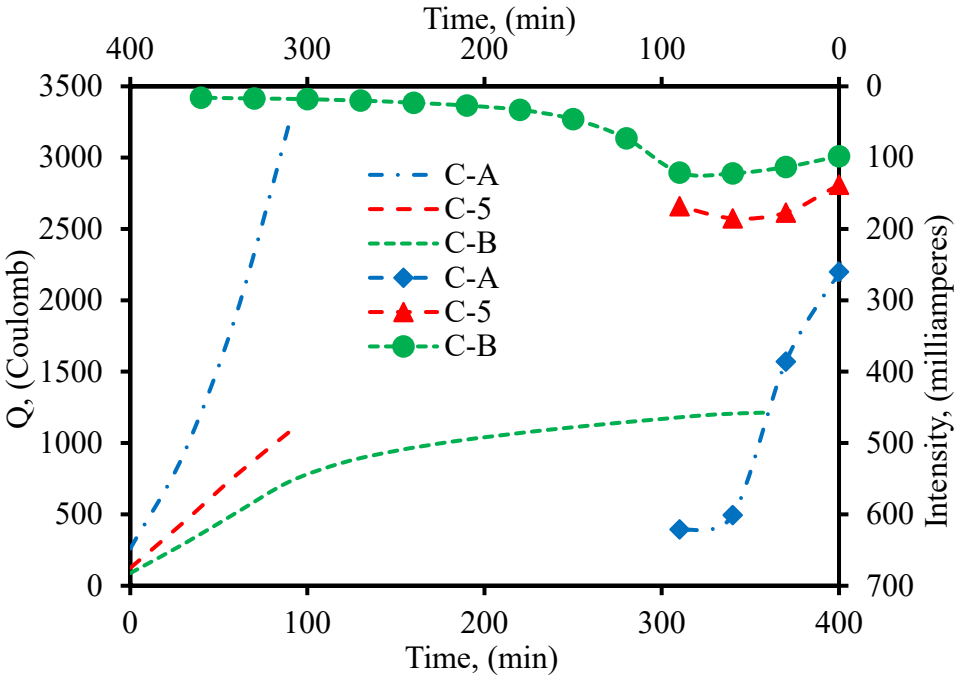

Figure 9. RCPT results of mixtures C-A, C-5, and C-B.

3.6. XRD

The efficiency of the crack healing could be expressed through the production of calcium carbonate precipitation. The recognized minerals of the three mixtures, including the control mixture, are illustrated in Figure 10. Peaks of calcite were observed at many angles for the AAS mixtures "C-5" and " C-B." These peaks indicate that the induced microbes could precipitate $CaCO_3$ crystals in both applications and undergo regular microbiological chemical reactions. *Bacillus subtilis* was capable of producing urease that helped in converting ($CO(NH_2)_2$) into ammonium (NH_4^+) and carbonate (CO_3^{2-}) [14,60]. This step led to elevating the pH level and increasing the carbonate concentration. The negatively charged carbonate ions produced from a series of biochemical ureolytic reactions attracted the positively charged calcium ions. These chemical reactions led to the formation of calcium carbonate ($CaCO_3$) at the cell surface, as explained in the following Equations (6)–(9) [15,60,61]:

$$CO(NH_2)_2 + H_2O \xrightarrow{\text{Urease}} NH_2COOH + NH_3 \quad (6)$$

$$NH_2COOH + H_2O \rightarrow NH_3 + H_2CO_3 \quad (7)$$

$$2NH_3 + 2H_2O \leftrightarrow 2NH_4^+ + 2OH^- \quad (8)$$

$$2OH^- + 2H_2CO_3 \leftrightarrow 2CO_3^{2-} + 2H_2O \quad (9)$$

$$Ca^{2+} + CO_3^{2-} \rightarrow CaCO_3 \downarrow \quad (10)$$

The calcite crystals filled the pores and the microcracks. Applying the bacterial suspension as a curing medium for AAS specimens could be verified by detecting the calcite compounds within the XRD of "C-B." Thus, the bacteria confirm its ability to act as a novel repair methodology and lay a solid foundation for presenting an environmentally friendly technique. Instead of incorporating bacteria solution during the fresh mixing, it could be applied externally in an efficient way to improve the external surface through healing the micro-cracks and filling the AAS pores and fissures, preventing the penetration of external attacks such as chlorides, carbon dioxide, and other hazardous substances to the

concrete degradation and steel reinforcement. The perception of calcite and the formation of different compounds such as sodalite, feldspar, and sodium alumino-silicate would appear more in the SEM and EDX performed in the mineralogy analyses in the next section.

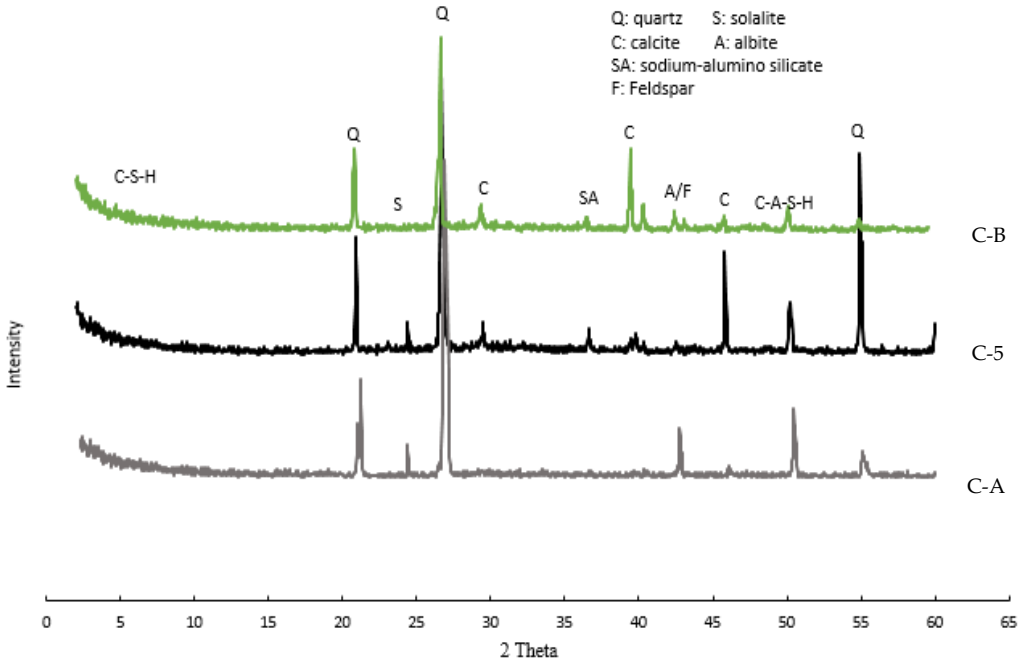

Figure 10. XRD of AAS mixtures: C-A, C-5, and C-B.

3.7. Mineralogy Analyses Using SEM and EDX

The SEM image of the control AAS mix "C-A" revealed the propagation of the shrinkage cracks within the alkali-activated composite. The volume instability property of AAS systems was highly confirmed in this image. The finer pore size distribution of AAS paste during nature and the complex hydration process increased the shrinkage vulnerability by 2–4 times compared to OPC concrete [14,51]. The percentage of the mesopores in AAS paste represents 74.0–82.0%, substantially higher than that in OPC paste, which represents 24.7–36.4% mesopores. Thus, the capillary tensile stress is caused by the pore distribution [60,62,63].

Furthermore, the lower Ca/Si ratio (1.1) in AAS concerning OPC paste Ca/Si ratio of 2.0 results in a different and complex hydration process [60]. The complex hydration process ends up incorporating alkali-metal ions produced by gel. After that, the presence of the alkali metal weakens the arrangement regularity of the C-S-H gel and makes the gel more susceptible to visco-elastic/visco-plastic characterization [14,60]. For the record, the Ca/Si ratio of the mixes here in the study is 0.43, 1.92, and 0.78 for mix C-A, C-5, and C-B, respectively. The ratio showed a low Ca/Si ratio (lower than 1.1), reflecting a similar alignment with the explanation stated by Yang et al. [60], except for mix C-B, which provided higher Ca due to the calcium carbonate perception possessed by the bacteria. Consequently, a healing agent was significantly required in the case of the alkali-activated systems. The SEM and EDX of the different ways of bacteria applications reflected promising results where more compact and denser microstructures were detected (Figure 11b,c) compared to the control mix (Figure 11a). Calcite crystals were observed in the AAS mixtures embedded with bacteria. These crystals were confirmed by the EDX analysis that revealed the existence of carbon atoms besides the calcium and oxygen atoms in the chemical composition (see Figure 11b,c), which emphasized the formation of $CaCO_3$ crystals. The SEM analysis agrees with those depicted by Jonkers et al. [41].

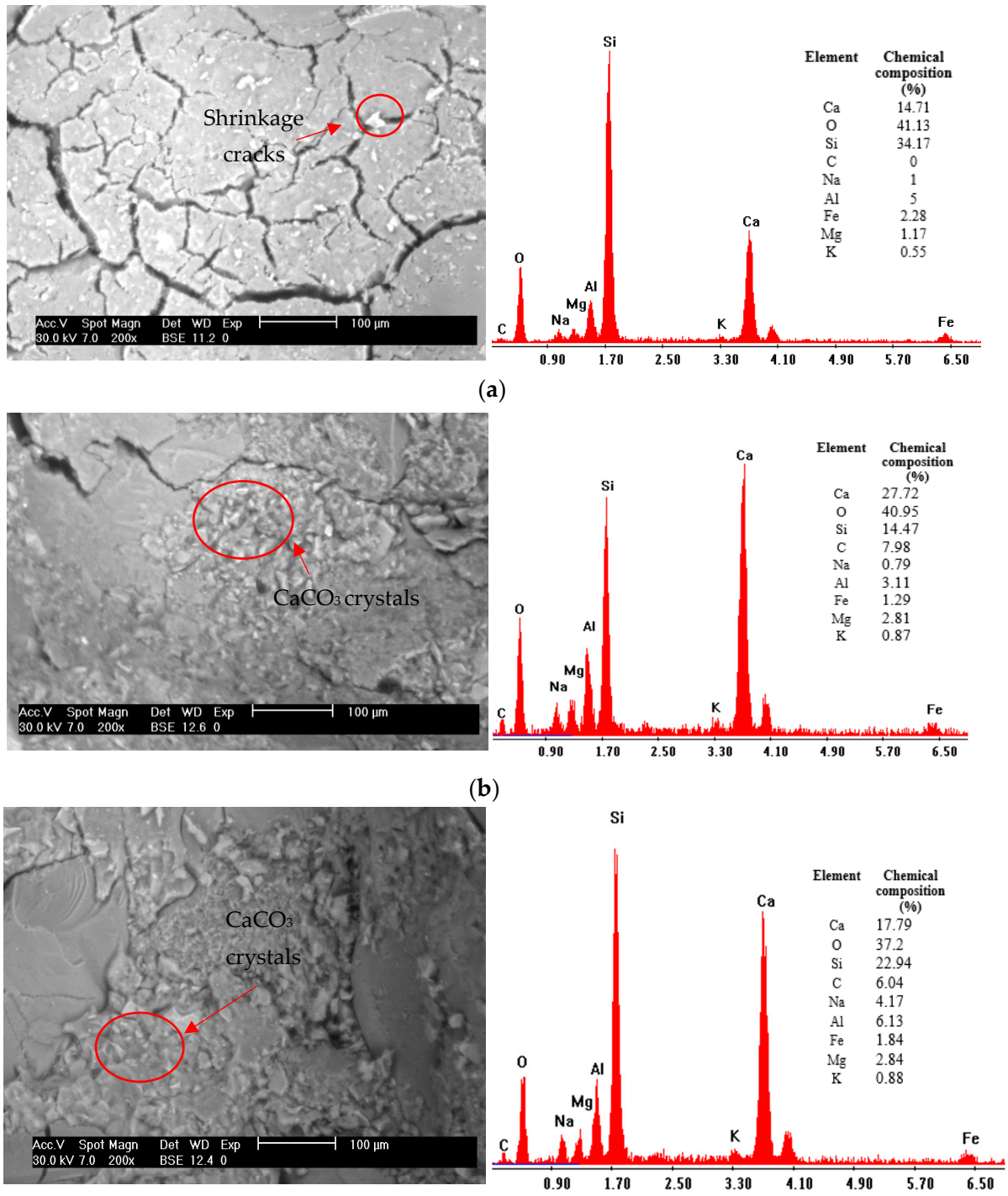

Figure 11. SEM images with EDX analysis of AAS mixtures: (**a**) C-A, (**b**) C-5, and (**c**) C-B.

Furthermore, it aligns with a study by Van Tittelboom et al. [22] on using *Bacillus sphaericus* for OPC crack repair, which conformed to enhancing water absorption porosity and strength properties. Therefore, the efficiency of the biological treatment was proved to be applied to AAS composites as a natural and pollution-free repair mechanism.

3.8. Surface Morphology and Crack Healing

Using *Bacillus subtilis* as an external repair technique performed well in AAS surface crack healing. The maximum healing crack width increased from 400 µm to 950 µm when

compared to immobilizing bacteria in the AAS fresh mix. *Bacillus subtilis* appeared to have the ability to perform microbial activities when used externally and precipitate calcium carbonate filling in the cracking area and surface pores. Figure 12 depicts the effective crack healing using *Bacillus subtilis* as a healing medium. The rate of healing seems to be 100 percentile in both cases of treatment, and this easily can be attributed to the calcite precipitation on the face in the case of mix C-B, where the curing with bacteria takes place, while direct inclusion of bacteria within the matrix would also possess the calcite early and on the surface, as in mix C-5. It should be mentioned that the rate of healing is calculated as mentioned by Mondal and Ghosh [36]. Hence, the durability properties showed a considerable enhancement after bacterial suspension treatment. It was apparent how chloride penetration was tested, where the rapid chloride test achieved superior results for C-B specimens compared to water-cured specimens, which was attributed to external pores and crack closure. These findings are consistent with previous studies [22,23] that confirmed the capability of applying *Bacillus subtilis* and *Bacillus sphaericus* as biological repair techniques. Microscopic photos are presented in Figure 12, capturing the progressive self-healing process of AAS specimens subjected to bacteria curing, and binary images show the cracks and their healing widths by filling the gaps.

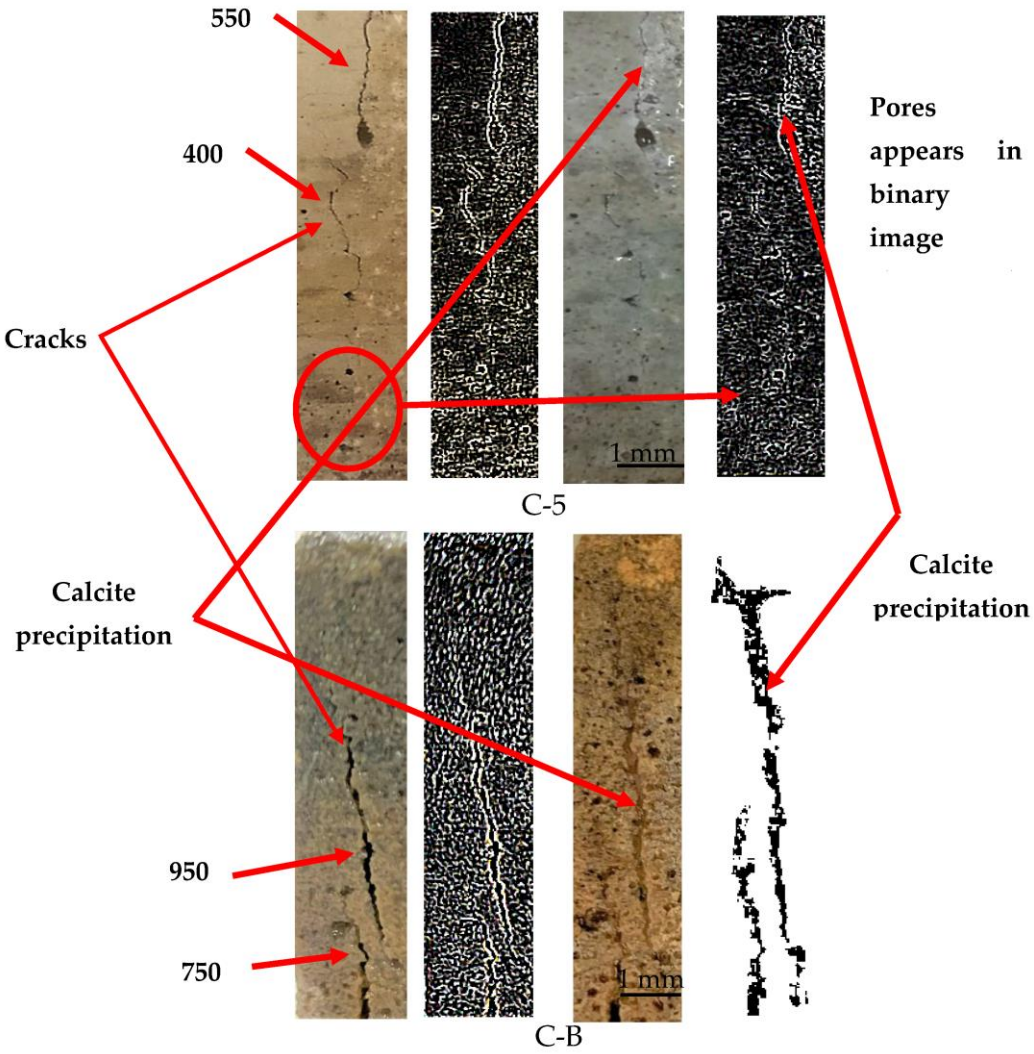

Figure 12. Visual surface morphology observations of the cracks before and after 28-day treatment of various bio mixtures: C-5 and C-B.

4. Limitations and Further Investigation

Using *Bacillus subtilis* can be a cost-effective solution due to its low cultivation requirements besides its ability to survive in dormant spore form for extended periods. Spores are inexpensive to produce and store, reducing the cost of bacterial incorporation into concrete compared to other biological methods such as encapsulation and hollow vessels [14,20,29,64]. However, some points shall be taken into consideration. One of these concerns is the long term, especially in dry or low-moisture areas. Moisture fluctuations impact bacterial activation, as *Bacillus subtilis* requires water to transition from a spore to an active form [29]. This could limit the self-healing potential of *Bacillus subtilis* in certain climates. Changes in moisture and pH alongside nutrient availability could lead to uncontrolled bacterial growth in undesired places, such as places with no cracks [29,64,65]. High pH can alter the enzymes' conformation, influencing their activity. It is worth mentioning that the pH level during concrete mixing is much more harsh for the bacteria (ranges from 12 to 13). Over time, this level declines to 9–10. The optimum pH range for *Bacillus subtilis* is between 6.5 and 8.5. But endospores could withstand this harsh condition. For that, *Bacillus subtilis* spores are recommended [64,65]. A further consideration is the scalability, cost, and logistics of applying this technology uniformly across the entire structure [66]. Also, the predictability of the mechanical properties while using the bacteria seems to be difficult due to the unpredictability of bacteria behavior, and the correlating compressive and flexural strengths need to be investigated as they are not similar to those assigned by codes or guidelines for further redesign and ensuring structural element integrity.

5. Conclusions

This study introduces an innovative approach to sustainable construction by proposing a biological solution as a novel green repair technology. Integrating sustainable binders such as slag and microorganisms leads the field into a new era of sustainable building materials. Two different mechanisms of incorporating *Bacillus subtilis* were assessed in this study. The first method directly incorporated microbe culture during the AAS mixing process, representing the traditional method of immobilizing bacteria. The second was adding bacteria into the curing media. The following points could be concluded based on this experimental work that evaluated the mechanical properties, including the compressive and flexural strengths, durability properties (water absorption, porosity, and chloride resistance), and the microstructure behavior through applying SEM, EDX, and XRD:

1. The direct method achieved 49.7% and 128% improvement in the compressive and flexural strengths. Utilizing bacteria culture in the curing medium for crack repair did not highly enhance the compressive strength. However, the flexural strength increased by 67%. The higher enhancement recorded in flexural strength was attributed to the direction of shrinkage crack propagation, which was perpendicular to the flexural tensile cracks.
2. The water absorption and porosity recorded enhanced results in both ways of bacteria application. Nevertheless, the enhancement increment was higher, with direct bacteria incorporation recorded at 42.0% and 32.1% compared to the microbial curing specimens, with percentages of 21.5% and 28.9% for the water absorption and porosity, respectively.
3. The microbial curing substantially improved the chloride resistance. It prolonged the resistance time by up to 6 h with low chloride penetration, where the specimens were classified as a perfect chloride-resistant composite, associated with the precipitation of the microbial-induced calcium carbonate on the external pores and cracks, which blocked mobile ion transmission.

4. SEM, EDX, and XRD emphasized the high potential of *Bacillus subtilis* to precipitate calcium carbonate in the AAS matrix when applied internally or externally.
5. Higher crack widths of healing were detected; the maximum healed crack width was 950 µm in microbial curing compared to 400 µm for the direct incorporation method. Hence, it could be introduced as an effective biological repair methodology.

The study explains how the self-healing bacteria would represent a new technique in treating cracks in the AAS, which is considered eco-friendly and would lead to more sustainability than demolishing or other repairing techniques that involve using deposited materials or removal of material that might create dust. The study also noted that the circular economy assessment would be supportive when studying the material itself and its reacting chemical component or mechanism of crack closure that could be initiated biogenetically or using chemicals to regain the strength and close cracks that assist in the protection of the building rather than any form of repair techniques and demolishing of materials.

Author Contributions: N.H.: Data curation, Formal analysis, Investigation, Methodology, Project administration, Resources, Software Programming, Validation, Visualization, Writing—original draft, Writing—review and editing Preparation. A.E.-N.: Data curation, Investigation, Methodology, Project administration, Resources, Software Programming, Supervision, Validation, Writing—review and editing Preparation. I.G.S.: Data curation, Investigation, Methodology, Project administration, Resources, Software Programming, Supervision, Validation, Writing—review and editing Preparation. All authors have read and agreed to the published version of the manuscript.

Funding: This research received no external funding.

Informed Consent Statement: Not applicable.

Data Availability Statement: Data will be made available upon request.

Acknowledgments: The authors would like to acknowledge the GUC Laboratory and the Technicians for their support and effort in conducting the testing required.

Conflicts of Interest: The authors declare no conflicts of interest.

Nomenclature

AAS	Alkali-activated slag
OPC	Ordinary Portland cement
$CaCO_3$	Calcium carbonate
$Na_2O\%$	Alkali dosage
Ms.	Modulus silicate
L/B	Liquid to binder
SEM	Spectroscopy electron microscope
EDX	Energy dispersive X-ray
XRD	X-ray diffraction
RCPT	Rapid chloride permeability test
ASTM	American Society for Testing Materials
ECP	Egyptian Code of Practice
C-S-H	Calcium silicate hydrates
C-S-A-H	Calcium silicate aluminate hydrates

References

1. Kayan, B.A.; Halim, I.A.; Mahmud, N.S. Green Maintenance for Heritage Buildings: An Appraisal Approach for St Paul's Church in Melaka, Malaysia. *Int. J. Technol.* **2018**, *9*, 1415. [CrossRef]
2. Klang, A.; Vikman, P.-Å.; Brattebø, H. Sustainable management of demolition waste—An integrated model for the evaluation of environmental, economic, and social aspects. *Resour. Conserv. Recycl.* **2003**, *38*, 317–334. [CrossRef]

3. Palomo, Á.; Kavalerova, E.; Fernández-Jiménez, A.; Krivenko, P.; García-Lodeiro, I.; Maltseva, O. A review on alkaline activation: New analytical perspectives. *Mater. Constr.* **2014**, *64*, e022. [CrossRef]
4. Hammad, N.; El-Nemr, A.; El-Deen Hasan, H. The performance of fiber GGBS-based alkali-activated concrete. *J. Build. Eng.* **2021**, *42*, 102464. [CrossRef]
5. Shaaban, I.; El Nemr, A.; Ahmed, H. Spotlight on mechanical properties of autogenic self-healing of concrete. In Proceedings of the 2nd International Summit on Civil, Structural, and Environmental Engineering, Florence, Italy, 18–20 March 2024. *in press*.
6. Hassanin, A.; El-Nemr, A.; Shaaban, H.F.; Saidani, M.; Shaaban, I.G. Coupling Behavior of Autogenous and Autonomous Self-Healing Techniques for Durable Concrete. *Int. J. Civ. Eng.* **2024**, *22*, 925–948. [CrossRef]
7. Melo Neto, A.A.; Cincotto, M.A.; Repette, W. Drying and autogenous shrinkage of pastes and mortars with activated slag cement. *Cem. Concr. Res.* **2008**, *38*, 565–574. [CrossRef]
8. Sierra-Beltran, M.G.; Jonkers, H.M.; Schlangen, E. Characterization of sustainable bio-based mortar for concrete repair. *Constr. Build. Mater.* **2014**, *67*, 344–352. [CrossRef]
9. Hilloulin, B.; Van Tittelboom, K.; Gruyaert, E.; De Belie, N.; Loukili, A. Design of polymeric capsules for self-healing concrete. *Cem. Concr. Compos.* **2015**, *55*, 298–307. [CrossRef]
10. Hendriks, C.A.; Worrell, E.; Price, L.; Martin, N.; Ozawa Meida, L.; de Jager, D.; Riemer, P. Emission reduction of greenhouse gases from the cement industry. *Greenh. Gas Control Technol.* **2019**, *4*, 939–944. [CrossRef]
11. Zhang, L.V.; Suleiman, A.R.; Mehdizadeh Allaf, M.; Marani, A.; Tuyan, M.; Nehdi, M.L. Crack self-healing in alkali-activated slag composites incorporating immobilized bacteria. *Constr. Build. Mater.* **2022**, *326*, 126842. [CrossRef]
12. Orinait, U.; Karalit, V.; Pal, M.; Ragulskis, M. Detecting Underwater Concrete Cracks with Machine Learning: A Clear Vision of a Murky Problem. *Appl. Sci.* **2023**, *13*, 7335. [CrossRef]
13. Rudawska, A.; Sarna-Bo, K.; Rudawska, A.; Olewnik-Kruszkowska, E.; Frigione, M. Biological Effects and Toxicity of Compounds Based on Cured Epoxy Resins. *Polymers* **2022**, *14*, 4915. [CrossRef]
14. Hammad, N.; Elnemr, A.; Shaaban, I.G. State-of-the-Art Report: The Self-Healing Capability of Alkali-Activated Slag (AAS) Concrete. *Materials* **2023**, *16*, 4394. [CrossRef] [PubMed]
15. Tan NP, B.; Keung, L.H.; Choi, W.H.; Lam, W.C.; Leung, H.N. Silica-based self-healing microcapsules for self-repair in concrete. *J. Appl. Polym. Sci.* **2015**, *133*, 43090. [CrossRef]
16. Han, N.-X.; Xing, F. A Comprehensive Review of the Study and Development of Microcapsule Self-Resilience Systems for Concrete Structures at Shenzhen University. *Materials* **2016**, *10*, 2. [CrossRef] [PubMed]
17. Shaaban, S.; Hammad, N.; Elnemr, A.; Shaaban, I.G. Efficiency of Bacteria-Based Self-Healing Mechanism in Concrete. *Mater. Sci. Forum* **2023**, *1089*, 135–143. [CrossRef]
18. Achal, V.; Mukerjee, A.; Sudhakara Reddy, M. Biogenic treatment improves the durability and remediates the cracks in concrete structures. *Constr. Build. Mater.* **2013**, *48*, 1–5. [CrossRef]
19. Qian, C.X.; Luo, M.; Ren, L.F.; Wang, R.X.; Li, R.Y.; Pan, Q.F.; Chen, H.C. Self-Healing and Repairing Concrete Cracks Based on Bio-Mineralization. *Key Eng. Mater.* **2014**, *629–630*, 494–503. [CrossRef]
20. Nguyen, T.H.; Ghorbel, E.; Fares, H.; Couture, A. Bacterial self-healing of concrete and durability assessment. *Cem. Concr. Compos.* **2019**, *104*, 103340. [CrossRef]
21. De Muynck, W.; Cox, K.; Belie, N.D.; Verstraete, W. Bacterial carbonate precipitation as an alternative surface treatment for concrete. *Constr. Build. Mater.* **2008**, *22*, 875–885. [CrossRef]
22. Van Tittelboom, K.; De Belie, N.; De Muynck, W.; Verstraete, W. Use of bacteria to repair cracks in concrete. *Cem. Concr. Res.* **2010**, *40*, 157–166, Elsevier BV. [CrossRef]
23. Prayuda, H. Repairing of Flexural Cracks on Reinforced Self-Healing Concrete Beam using Bacillus Subtillis Bacteria. *Int. J. Integr. Eng.* **2020**, *12*, 300–309.
24. Ramachandran, S.K.; Ramakrishnan, V.; Bang, S.S. Remediation of Concrete Using Microorganisms. *ACI Mater. J.* **2001**, *98*, 3–9. [CrossRef]
25. Nosouhian, F.; Mostofinejad, D.; Hasheminejad, H. Concrete Durability Improvement in a Sulfate Environment Using Bacteria. *J. Mater. Civ. Eng.* **2016**, *28*, 04015064. [CrossRef]
26. Hosseini Balam, N.; Mostofinejad, D.; Eftekhar, M. Use of carbonate precipitating bacteria to reduce water absorption of aggregates. *Constr. Build. Mater.* **2017**, *141*, 565–577. [CrossRef]
27. Khaliq, W.; Ehsan, M.B. Crack healing in concrete using various bio influenced self-healing techniques. *Constr. Build. Mater.* **2016**, *102*, 349–357. [CrossRef]
28. *ECP 203-2007*; Egyptian Code for Design and Construction of Reinforced Concrete Structures. Ministry of Housing, Utilities, and Urban Development of Egypt: Cairo, Egypt, 2007.
29. Espitia-Nery, M.E.; Corredor-Pulido, D.E.; Castano-Oliveros, P.A. Mechanisms of encapsulation of bacteria in self-healing concrete: Review. *DYNA* **2019**, *86*, 17–22. [CrossRef]

30. Andalib, R.; Abd Majid, M.Z.; Hussin, M.W.; Ponraj, M.; Keyvanfar, A.; Mirza, J.; Lee, H.-S. Optimum concentration of Bacillus megaterium for strengthening structural concrete. *Constr. Build. Mater.* **2016**, *118*, 180–193. [CrossRef]
31. Vaezi, M.; Zareei, S.A.; Jahadi, M. Recycled microbial mortar: Effects of bacterial concentration and calcium lactate content. *Constr. Build. Mater.* **2020**, *234*, 117349. [CrossRef]
32. Mondal, S.; Ghosh, A. Investigation into the optimal bacterial concentration for compressive strength enhancement of microbial concrete. *Constr. Build. Mater.* **2018**, *183*, 202–214. [CrossRef]
33. Bayati, M.; Saadabadi, L.A. Efficiency of bacteria-based self-healing method in alkali-activated slag (AAS) mortars. *J. Build. Eng.* **2021**, *42*, 102492. [CrossRef]
34. *ASTM C109*; Standard Test Method of Compressive Strength of Hydraulic Cement Mortars (Using 2-in. or [50 mm] Cube Specimens). ASTM International: West Conshohocken, PA, USA, 2020.
35. *ASTM C348-21*; Standard Test Method for Flexural Strength of Hydraulic-Cement Mortars. ASTM International: West Conshohocken, PA, USA, 2021.
36. Mondal, S.; Ghosh, A. Spore-forming Bacillus subtilis vis-à-vis non-spore-forming Deinococcus radiodurans, a novel bacterium for self-healing of concrete structures: A comparative study. *Constr. Build. Mater.* **2021**, *266*, 121122. [CrossRef]
37. *ASTM C642-21*; Standard Test Method for Density, Absorption, and Voids in Hardened Concrete. ASTM International: West Conshohocken, PA, USA, 2022.
38. *ASTM C1202-19*; Standard Test Method for Electrical Indication of Concrete's Ability to Resist Chloride Ion Penetration. ASTM International: West Conshohocken, PA, USA, 2022.
39. *AASHTO-T277*; Standard Method of Test for Electrical Indication of Concrete's Ability to Resist Chloride Ion Penetration. AASHTO: Washington, DC, USA, 2023.
40. Jadhav, U.U.; Lahoti, M.; Chen, Z.; Qiu, J.; Cao, B.; Yang, E.-H. Viability of bacterial spores and crack healing in bacteria-containing geopolymer. *Constr. Build. Mater.* **2018**, *169*, 716–723. [CrossRef]
41. Jonkers, H.M.; Thijssen, A.; Muyzer, G.; Copuroglu, O.; Schlangen, E. Application of bacteria as self-healing agent for the development of sustainable concrete. *Ecol. Eng.* **2010**, *36*, 230–235. [CrossRef]
42. Krishnapriya, S.; Venkatesh Babu, D.L.; Prince Arulraj, G. Isolation and identification of bacteria to improve the strength of concrete. *Microbiol. Res.* **2015**, *174*, 48–55. [CrossRef] [PubMed]
43. Ghosh, S.; Biswas, M.; Chattopadhyay, B.D.; Mandal, S. Microbial activity on the microstructure of bacteria-modified mortar. *Cem. Concr. Compos.* **2009**, *31*, 93–98. [CrossRef]
44. Sunil Pratap Reddy, S.; Seshagiri Rao, M.V.; Aparna, P.; Sasikala, C. Performance of standard grade bacterial concrete. *Asian J. Civ. Eng. (Build. Hous.)* **2010**, *11*, 43–55.
45. Siddique, R.; Singh, K.; Kunal Singh, M.; Corinaldesi, V.; Rajor, A. Properties of bacterial rice husk ash concrete. *Constr. Build. Mater.* **2016**, *121*, 112–119. [CrossRef]
46. Siddique, R.; Nanda, V.; Kunal Kadri, E.-H.; Iqbal Khan, M.; Singh, M.; Rajor, A. Influence of bacteria on compressive strength and permeation properties of concrete made with cement baghouse filter dust. *Constr. Build. Mater.* **2015**, *106*, 461–469. [CrossRef]
47. Chahal, N.; Siddique, R.; Rajor, A. Influence of bacteria on the compressive strength, water absorption, and rapid chloride permeability of fly ash concrete. *Constr. Build. Mater.* **2012**, *28*, 351–356. [CrossRef]
48. Bhaskar, S.; Hossain, K.M.A.; Lachemi, M.; Wolfaardt, G.; Kroukamp, M.O. Effect of self-healing on strength and durability of zeolite-immobilized bacterial cementitious mortar composites. *Cem. Concr. Compos.* **2017**, *82*, 23–33. [CrossRef]
49. Modesti, L.A.; De Vargas, A.S.; Schneider, E.L. Repairing Concrete with Epoxy Adhesives. *Int. J. Adhes. Adhes.* **2020**, *101*, 102645. [CrossRef]
50. Santos, P.; Júlio, E.N.B.S. Factors Affecting Bond between New and Old Concrete. *ACI Mater. J.* **2011**, *108*, 449–456. [CrossRef]
51. Fang, G.; Bahrami, H.; Zhang, M. Mechanisms of autogenous shrinkage of alkali-activated fly ash-slag pastes cured at ambient temperature within 24 h. *Constr. Build. Mater.* **2018**, *171*, 377–387. [CrossRef]
52. Hassan, A.; ElNemr, A.; Goebel, L.; Koenke, C. Effect of hybrid polypropylene fibers on mechanical and shrinkage behavior of alkali-activated slag concrete. *Constr. Build. Mater.* **2024**, *411*, 134485. [CrossRef]
53. Siddique, R.; Jameel, A.; Singh, M.; Barnat-Hunek, D.; Kunal Aït-Mokhtar, A.; Belarbi, R.; Rajor, A. Effect of bacteria on strength, permeation characteristics and micro-structure of silica fume concrete. *Constr. Build. Mater.* **2017**, *142*, 92–100. [CrossRef]
54. Osio-Norgaard, J.; Gevaudan, J.P.; Srubar, W.V., III. A review of chloride transport in alkali-activated cement paste, mortar, and concrete. *Constr. Build. Mater.* **2018**, *186*, 191–206. [CrossRef]
55. Ye, H.; Huang, L.; Chen, Z. Influence of activator composition on the chloride binding capacity of alkali-activated slag. *Cem. Concr. Compos.* **2019**, *104*, 103368. [CrossRef]
56. Ma, Q.; Nanukuttan, S.V.; Basheer, P.A.M.; Bai, Y.; Yang, C. Chloride transport and the resulting corrosion of steel bars in alkali-activated slag concrete. *Mater. Struct.* **2015**, *49*, 3663–3677. [CrossRef]
57. Zhang, J.; Ma, Y.; Hu, J.; Wang, H.; Zhang, Z. Review on chloride transport in alkali-activated materials: Role of precursors, activators, and admixtures. *Constr. Build. Mater.* **2022**, *328*, 127081. [CrossRef]

58. Balcikanli, M.; Ozbay, E. Optimum design of alkali-activated slag concretes for the low oxygen/chloride ion permeability and thermal conductivity. *Compos. Part B Eng.* **2016**, *91*, 243–256. [CrossRef]
59. Hu, X.; Shi, C.; Shi, Z.; Zhang, L. Compressive strength, pore structure, and chloride transport properties of alkali-activated slag/fly ash mortars. *Constr. Build. Mater.* **2019**, *104*, 103392. [CrossRef]
60. Yang, L.Y.; Jia, Z.J.; Zhang, Y.M.; Dai, J.G. Effects of nano-TiO2 on strength, shrinkage, and microstructure of alkali-activated slag pastes. *Cem. Concr. Compos.* **2015**, *57*, 1–7. [CrossRef]
61. Wu, M.; Johannesson, B.; Geiker, M. A review: Self-healing in cementitious materials and engineered cementitious composite as a self-healing material. *Constr. Build. Mater.* **2012**, *28*, 571–583. [CrossRef]
62. Hammad, N.; Elnemr, A.; Shaaban, I.G. The efficiency of calcium oxide on microbial self-healing activity in alkali-activated slag (AAS). *Appl. Sci.* **2024**, *14*, 5299. [CrossRef]
63. Aydin, S.; Baradan, B. Effect of activator type and content on properties of alkali-activated slag mortars. *Compos. Part B Eng.* **2014**, *57*, 166–172. [CrossRef]
64. Wang, P.Y.; Mal, J.; Sandak, A.; Luo, L.; Jian, J.; Pradhan, N. Advances in microbial self-healing concrete: A critical review of mechanisms, developments, and future direction. *Sci. Total Environ.* **2024**, *947*, 17455. [CrossRef] [PubMed]
65. Mahmood, F.; Kashif Ur Rehman, S.; Jameel, M.; Riaz, N.; Javed, M.F.; Salmi, A.; Awad, Y.A. Self-Healing Bio-Concrete Using Bacillus subtilis Encapsulated in Iron Oxide Nanoparticles. *Materials* **2022**, *15*, 7731. [CrossRef]
66. Rahman, M.M.; Hora, R.N.; Ahenkorah, I.; Beecham, S.; Karim, M.R.; Iqbal, A. State-of-the-art review of Microbial-Induced Calcite Precipitation and Its Sustainability in Engineering Applications. *Sustainability* **2020**, *12*, 6281. [CrossRef]